Electronic structure of Sn/Cu(100)-$(2\sqrt{2} \times 2\sqrt{2})R45^{\circ}$

2009 J. Phys.: Condens. Matter 21 055001

(http://iopscience.iop.org/0953-8984/21/5/055001)

J. Phys.: Condens. Matter **21** (2009) 055001 (6pp) doi:10.1088/0953-8984/21/5/055001

Electronic structure of Sn/Cu(100)-$(2\sqrt{2} \times 2\sqrt{2})$R45°

J Martínez-Blanco[1], V Joco[1], J Fujii[2], P Segovia[1] and E G Michel[1]

[1] Departamento de Física de la Materia Condensada and Instituto Universitario de Ciencia de Materiales 'Nicolás Cabrera', Universidad Autónoma de Madrid, E-28049 Madrid, Spain
[2] TASC National Laboratory, CNR-INFM, S.S. 14, km 163.5, I-34012 Trieste, Italy

E-mail: enrique.garcia.michel@uam.es

Received 1 February 2008, in final form 2 October 2008
Published 16 December 2008
Online at stacks.iop.org/JPhysCM/21/055001

Abstract
We present measurements of the Fermi surface and underlying band structure of Sn/Cu(100)-$(2\sqrt{2} \times 2\sqrt{2})$R45°. This phase is observed for a coverage of 0.60–0.65 monolayers. Its electronic structure is characterized by a free-electron-like surface band folded with the reconstruction periodicity. At variance with other surface phases of Sn on Cu(100), no temperature-induced phase transition is observed for this phase from 100 K up to the desorption of Sn.

(Some figures in this article are in colour only in the electronic version)

1. Introduction

The interaction of various metals with the Cu(100) surface has been widely investigated due to the interest in metal-on-metal epitaxial growth. In the case of group III and IV metals, a large surface mobility [1] facilitates the formation of ordered structures. The superstructures formed when Sn is deposited on Cu(100) have been investigated using different techniques, since the first report by Argile and Rhead [2], including low-energy electron diffraction, scanning tunneling microscopy and thermal energy helium scattering [3–8]. The large lattice mismatch between Sn and Cu(100) explains in part the many different superstructures observed when Sn is deposited at room temperature in the monolayer (ML) and submonolayer coverage range: p(2 × 2) (for 0.2 ML), p(2 × 6) (for 0.33 ML), $\begin{pmatrix} -4 & 2 \\ 0 & 4 \end{pmatrix}$ (for 0.45 ML, equivalent to a c(4 × 8)), $(3\sqrt{2} \times \sqrt{2})$R45° (for 0.5 ML) and finally $(2\sqrt{2} \times 2\sqrt{2})$R45° (for 0.65 ML). The thermal stability of these phases has been analyzed by us before [6]. We found two different temperature-induced reversible phase transitions, both at approximately the same temperature of 360 K: $(3\sqrt{2} \times \sqrt{2})$R45° ↔ $(\sqrt{2} \times \sqrt{2})$R45° and $\begin{pmatrix} -4 & 2 \\ 0 & 4 \end{pmatrix}$ ↔ p(2 × 2).

Nakagawa *et al* [9, 10] have reported that an In overlayer of 0.5 ML on Cu(100) exhibits a reversible phase transition at ∼350 K from a $(9\sqrt{2} \times 2\sqrt{2})$R45° reconstruction at low temperature to a $(\sqrt{2} \times \sqrt{2})$R45° reconstruction at high temperature. Several other structures are found for other coverages, and there is an additional temperature-induced phase transition from $(2\sqrt{2} \times 2\sqrt{2})$R45° to p(2 × 2) (for 0.6 ML) [11]. The most interesting feature of both phase transitions is that they can be interpreted as the stabilization of a surface CDW by Fermi surface nesting. These findings have triggered the interest in related surface systems. In particular, the phase transition mentioned above for Sn/Cu(100)-$(3\sqrt{2} \times \sqrt{2})$R45° to $(\sqrt{2} \times \sqrt{2})$R45° above ∼360 K presents similar features. Thus, the Fermi contour of this phase exhibits an almost perfect nesting vector to generate the triple periodicity observed at lower temperatures. The electronic properties of this phase transition have been analyzed in detail in [12, 13].

Besides the general interest of surface phase transitions [14–16], the phase transitions described above exhibit interesting common features, such as a large bandgap and a large coherence length [17], making them examples of a new paradigm of two-dimensional CDW systems [18, 19]. However, while In/Cu(100)-$(2\sqrt{2} \times 2\sqrt{2})$R45° is stabilized by nesting and gapping in the p(2 × 2) Fermi surface, the equivalent Sn/Cu(100)-$(2\sqrt{2} \times 2\sqrt{2})$R45° phase does not seem to exhibit any phase transition. The purpose of this paper is to investigate the electronic properties of Sn/Cu(100)-$(2\sqrt{2} \times 2\sqrt{2})$R45° in order to understand the different behavior observed. We report here angle-resolved photoemission spectroscopy (ARPES) results, complemented with low-energy electron diffraction (LEED) for Sn/Cu(100)-$(2\sqrt{2} \times 2\sqrt{2})$R45°. We find that this phase also presents a free-electron-like surface band, but the Fermi momentum is not related to the structural periodicity. A zone edge bandgap is

seen at a binding energy (BE) of ~ -1.6 eV, and it is expected to approach the Fermi energy near the $\overline{\mathrm{M}}$ point of the $(2\sqrt{2} \times 2\sqrt{2})$R45° surface Brillouin zone. However, no evidence of bandgap opening is detected in the Fermi contour. We conclude that the lack of Fermi bandgap is due to the different filling of the surface band with respect to the analogous In/Cu(100), where a bandgap is indeed detected.

2. Experiment

The experiments were made in a ultrahigh vacuum chamber permanently mounted at the APE beamline of Elettra Laboratory (Trieste, Italy). The energy and angle resolutions are set to 60 meV/0.12°. Fermi surface mapping and most measurements were performed at constant photon energy (27 eV), which is a favorable value due to restrictions from the bulk electronic structure [13]. The surface and bulk bands were mapped in a window of approximately 4 eV below the Fermi energy using a Scienta electron analyzer. The polarization plane of the light was horizontal and coincided with the measuring plane. An energy window of 1.5 eV was mapped with high resolution in order to probe the electronic states closer to the Fermi energy. Photoemission intensity is represented in a gray scale, where white corresponds to high intensity. Constant binding energy surfaces were mapped for approximately one-half of the reciprocal space, and were mirrored according to the fourfold symmetry of Cu(100). The Cu(100) surface is prepared by Ar sputtering and annealing, following standard procedures until a sharp (1×1) LEED pattern was observed. The quality of the surface was checked by measuring the narrow d-like surface state of odd symmetry at $\overline{\mathrm{M}}$. Sn was dosed from a Knudsen cell. The $(2\sqrt{2} \times 2\sqrt{2})$R45° structure is produced by deposition of 0.60–0.65 ML of Sn at 300 K. This procedure provides high quality LEED patterns with low background. The coverage is calibrated from the sequence of structures below 1 ML [3, 6] and from the Sn 5d/Cu 3d intensity ratio. The sequence of structures is a sensitive tool to determine the coverage, because residual intensity from other structures is observed in the LEED pattern when the coverage exceeds or is below the right value corresponding to a particular structure. Symmetry points are referred to the Cu(100) surface Brillouin zone, unless otherwise stated. k_x corresponds to the $\overline{\Gamma\mathrm{M}}$ direction in this paper.

3. Results and discussion

Figure 1 summarizes the thermal behavior of the $(2\sqrt{2} \times 2\sqrt{2})$R45° structure. The figure also includes results for the $(3\sqrt{2} \times \sqrt{2})$R45° phase to facilitate a comparison [6]. In the case of the $(3\sqrt{2} \times \sqrt{2})$R45° phase, a fully reversible phase transition to a $(\sqrt{2} \times \sqrt{2})$R45° phase is observed at 360 K. No significant hysteresis is detected within experimental accuracy and the phase transition can be crossed many times without degrading. In contrast, the $(2\sqrt{2} \times 2\sqrt{2})$R45° pattern is irreversibly destroyed upon heating above 350 K. Then, a low quality $(\sqrt{2} \times \sqrt{2})$R45° is observed, but after cooling down, a $(3\sqrt{2} \times \sqrt{2})$R45° pattern appears. As the coverage difference

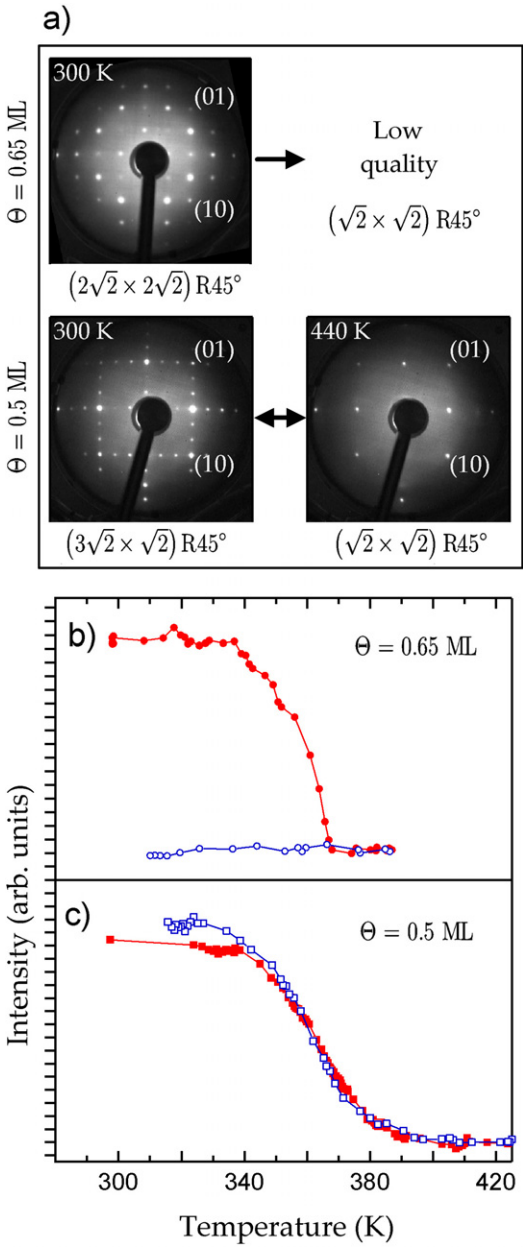

Figure 1. (a) LEED patterns at 70 eV for 0.5 ML and at 104 eV for 0.65 ML Sn/Cu(100) at 300 K (left) and 440 K (right). For 0.5 ML, the $(3\sqrt{2} \times \sqrt{2})$R45° undergoes a phase transition to $(\sqrt{2} \times \sqrt{2})$R45°. For 0.65 ML, the $(2\sqrt{2} \times 2\sqrt{2})$R45° observed at room temperature is transformed into a low quality $(\sqrt{2} \times \sqrt{2})$R45°, see the text for details. (b) Integrated intensity of the (3/4, 1/4) reflection specific to the $(2\sqrt{2} \times 2\sqrt{2})$R45° phase. The intensity is not recovered upon cooling down and the $(2\sqrt{2} \times 2\sqrt{2})$R45° is destroyed by heating above 350 K. (c) Same for the (5/6, 5/6) reflection specific to the $(3\sqrt{2} \times \sqrt{2})$R45° phase versus temperature, showing the full reversibility of the transition. In both cases, heating up is represented by red filled circles and cooling down by blue open circles.

between both phases is small (0.65 versus 0.5 ML), this suggests that the $(2\sqrt{2} \times 2\sqrt{2})$R45° is unstable upon heating above 350 K, and that it decomposes into a $(3\sqrt{2} \times \sqrt{2})$R45° and probably disordered Sn atoms, as the temperatures reached are too low for Sn desorption and the solubility in the bulk is

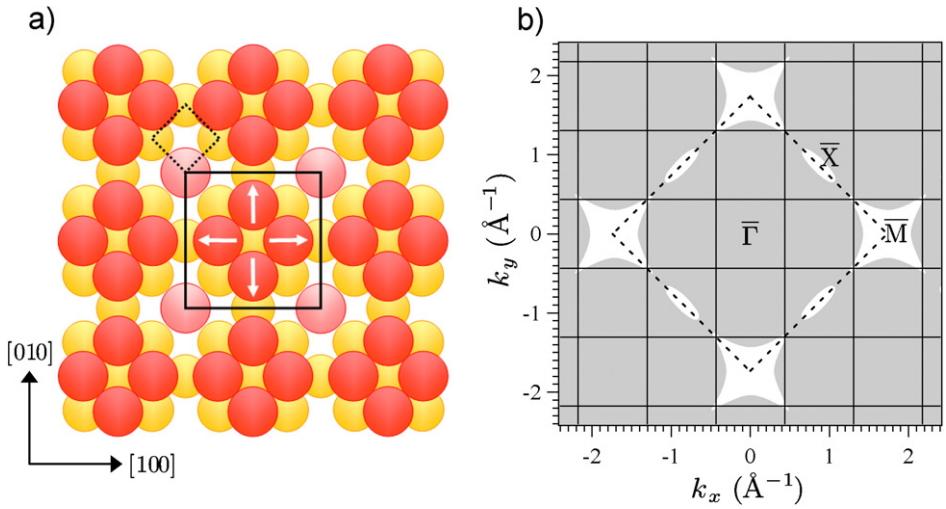

Figure 2. (a) Atomic model for the $(2\sqrt{2} \times 2\sqrt{2})$R45° (from [8]). Yellow (small and light gray) circles are last layer Cu atoms, red/pink (large and light/dark gray) circles correspond to inequivalent Sn atoms. The dashed lines highlight the (1×1) substrate unit cell and continuous lines the primitive $(2\sqrt{2} \times 2\sqrt{2})$R45° unit cell. Arrows indicate the direction of atomic displacements from fourfold hollow sites. (b) Cu(100) reciprocal space, where dashed lines mark the (1×1) Brillouin zone and continuous lines the $(2\sqrt{2} \times 2\sqrt{2})$R45° Brillouin zone. The unshaded area denotes Cu(100) bulk bandgaps.

very small. The temperature range down to 100 K was also probed and no additional phase transition could be observed.

Figure 2 shows the atomic model of the $(2\sqrt{2}\times2\sqrt{2})$R45° superstructure, taken from [8]. A similar (but not identical) structural model has been found for In/Cu(100)-$(2\sqrt{2} \times 2\sqrt{2})$R45° on the basis of LEED [20], surface x-ray diffraction (SXRD) [21] and STM [11]. The $(2\sqrt{2} \times 2\sqrt{2})$R45° unit cell contains five Sn atoms (thus giving a nominal coverage of $5/8 = 0.625$ ML) in two inequivalent adsorption sites: the four Sn atoms forming the central tetramer occupy a fourfold hollow site (coverage $4/8 = 0.5$ ML) and the corner Sn atom (coverage $1/8 = 0.125$ ML) occupies an ontop site. Interestingly, the $(2\sqrt{2} \times 2\sqrt{2})$R45° structure is irreversibly destroyed by heating above 350 K. After cooling down a $(3\sqrt{2} \times \sqrt{2})$R45° phase is recovered. As the coverage for this phase is exactly 0.5 ML, this behavior suggests that the 0.125 ML of Sn atoms occupying ontop sites are less tightly bound, or even mobile, as they are not imaged in STM pictures [8], and that they might be removed from the surfaces, or at least from its ordered parts, by a slight annealing.

A scheme of the relevant reciprocal space area appears in figure 2. The projection of Cu electronic bulk bands along the (100) direction leaves absolute bandgaps around the $\overline{M}$ and $\overline{X}$ points. Sn-induced surface states have a pure surface character within the bandgap regions. Outside this area, Sn surface resonances can be detected as well, but in general they are partially mixed with bulk states. In previous publications we have shown that the $(\sqrt{2} \times \sqrt{2})$R45° phase is characterized by a prominent Sn-induced metallic surface band, with a nearly free-electron behavior, whose crossing points span a nesting vector in agreement with the $(3\sqrt{2} \times \sqrt{2})$R45° periodicity [12, 13]. The electronic structure of the $(2\sqrt{2} \times 2\sqrt{2})$R45° phase investigated here also exhibits a surface state of similar characteristics.

Figure 3 shows ARPES measurements along the $\overline{\Gamma M}$ direction ($\phi = 0°$) and for azimuthal angles ϕ up to 12° off. The band observed in figure 3 is an Sn-induced surface state, of similar origin and properties as the surface

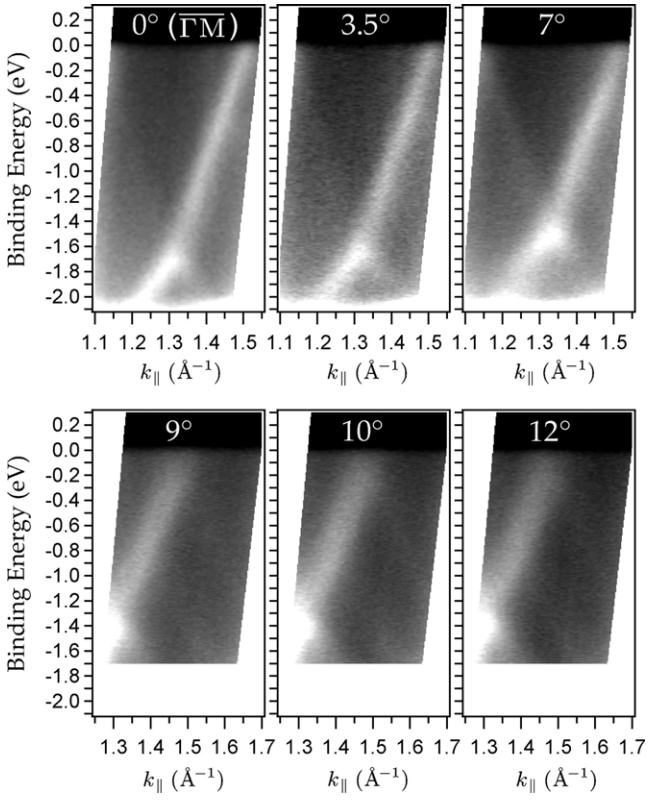

Figure 3. Valence band structure in gray scale measured with $h\nu = 27$ eV versus parallel momentum ($k_{\|}$) for the $(2\sqrt{2} \times 2\sqrt{2})$R45° phase for a range of azimuthal angles close to the $\overline{\Gamma M}$ direction. Note a prominent surface band crossing the Fermi energy. At lower binding energies an avoided-crossing zone edge bandgap is observed. A weak backfolded band generates the gap (see, for instance, the data for 7°).

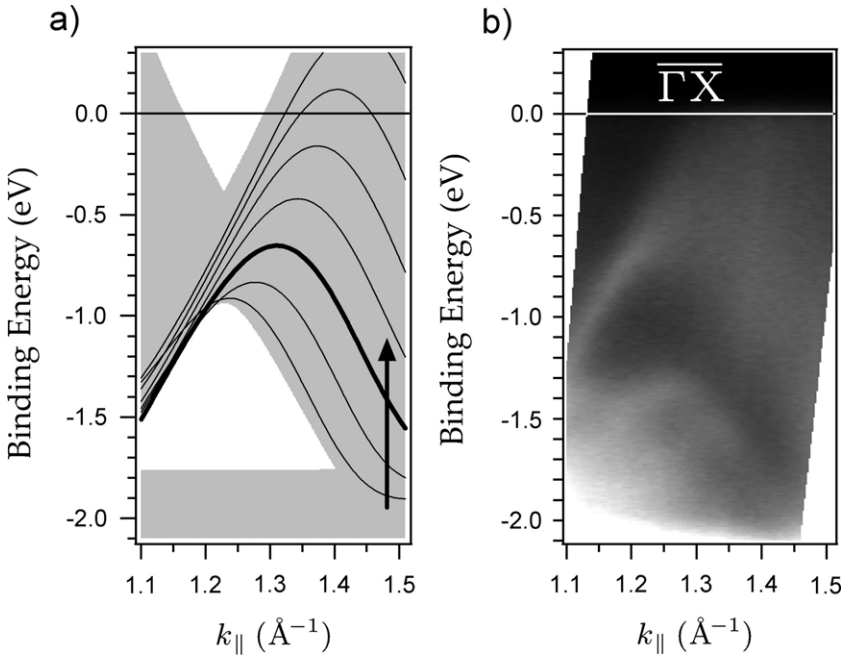

Figure 4. (a) Calculated dispersion of the Cu sp bulk band along $\overline{\Gamma X}$ for different photon energies from 25 up to 31 eV in 1 eV steps (thick line: 27 eV) [22]. Unshaded areas denote Cu(100) bulk bandgaps. (b) Valence band structure in gray scale for $h\nu = 27$ eV along the $\overline{\Gamma X}$ direction in the region of the $\overline{X}$ point. See the text for details.

state bands observed for Sn/Cu(100)-$(3\sqrt{2} \times \sqrt{2})$R45° and In/Cu(100) [9–11]. It exhibits a free-electron-like behavior and crosses the Fermi energy for a Fermi momentum of (1.50 ± 0.02) Å^{-1} along $\overline{\Gamma M}$. The dispersion of this surface band is similar to the dispersion found for the $(\sqrt{2} \times \sqrt{2})$R45° structure [12], but the Fermi momentum is larger. This agrees well with the larger Sn coverage, which gives rise to a larger filling of the surface band. On the other hand, as shown in figure 3, the band crosses the Brillouin zone edge (at 1.31 Å^{-1}) for a binding energy of ~ -1.6 eV, giving rise to an avoided-crossing zone edge bandgap. The backfolded band is centered at another $\overline{\Gamma}$ point along the $\overline{\Gamma M}$ direction (see also figure 5). Its intensity is rather weak, but it can be distinguished in some of the energy versus momentum data in figure 3. Several features of the zone edge gap deserve a comment. First, the bandgap lies in the occupied part of the band structure and thus it does not involve any energetic gain. This is at variance with the bandgap observed for the $(3\sqrt{2} \times \sqrt{2})$R45° phase, which lies right at the Fermi energy. Second, the bandgap approaches the Fermi energy as we go away from the $\overline{\Gamma M}$ direction. This behavior is easily explained if we consider two paraboloids representing the quasi-free-electron-like dispersion of the surface state, centered at $\overline{\Gamma}_{(0,0)}$ and $\overline{\Gamma}_{(3,0)}$ of the $(2\sqrt{2} \times 2\sqrt{2})$R45° structure (see figure 5). Note that, in principle, we may expect that the surface band is folded with the full $(2\sqrt{2} \times 2\sqrt{2})$R45° periodicity, and thus such a paraboloid should be repeated in each of the $\overline{\Gamma}$ points of the $(2\sqrt{2} \times 2\sqrt{2})$R45° structure. It is clear, however, that the intensity of the folding is, in general, weak, with a few exceptions, as it depends on the strength of the periodic potential related to the superstructure and matrix element effects.

Figure 4 shows the band dispersion along the $\overline{\Gamma X}$ high symmetry direction, in the region around the $\overline{X}$ point, for a photon energy of 27 eV. The data are compared to tight binding calculations for the bulk band structure of Cu(100) [22]. The most intense band observed in figure 4 (dispersing from -1.2 eV at 1.1 Å^{-1} towards the Fermi energy) corresponds to the bulk sp band. The band becomes broadened as it passes the $\overline{X}$ point at $k_{\parallel} = 1.23$ Å^{-1}. The band observed around the $\overline{X}$ point for -1.5 eV binding energy probably corresponds to the surface state band, as this area lies within a bulk bandgap. A similar band was observed for the $(3\sqrt{2} \times \sqrt{2})$R45° structure [13], where it was also attributed to a surface state band.

Figure 5 shows the Fermi surface and constant energy surfaces for BEs down to -0.6 eV for the $(2\sqrt{2} \times 2\sqrt{2})$R45° reconstruction, mapped at 300 K using a photon energy of 27 eV. The intensity is represented in logarithmic scale to enhance the contrast. The Cu(100) band structure presents bandgaps around $\overline{X}$ and $\overline{M}$ points, so beyond these areas we expect that bulk Cu bands contribute also to the Fermi contours. The red lines correspond to the Cu(100) sp band constant energy surfaces: for a detailed analysis we refer the reader to [13]. The constant energy surface of Cu(100) is observed mainly at two locations: the crossing along $\overline{\Gamma M}$ (at 1.1 Å^{-1}) and a range close to the $\overline{X}$ point. The rest of the intensity observed is related exclusively to the Sn-induced surface state, which generates the outer circle in the range 1.2 Å^{-1} $\leqslant k_x \leqslant$ 1.6 Å^{-1}. The almost circular shape directly reveals that the surface state behaves, to a very good approximation, as a nearly free-electron, two-dimensional surface band. Following the free-electron model we can compare electron filling and differences in Fermi momentum

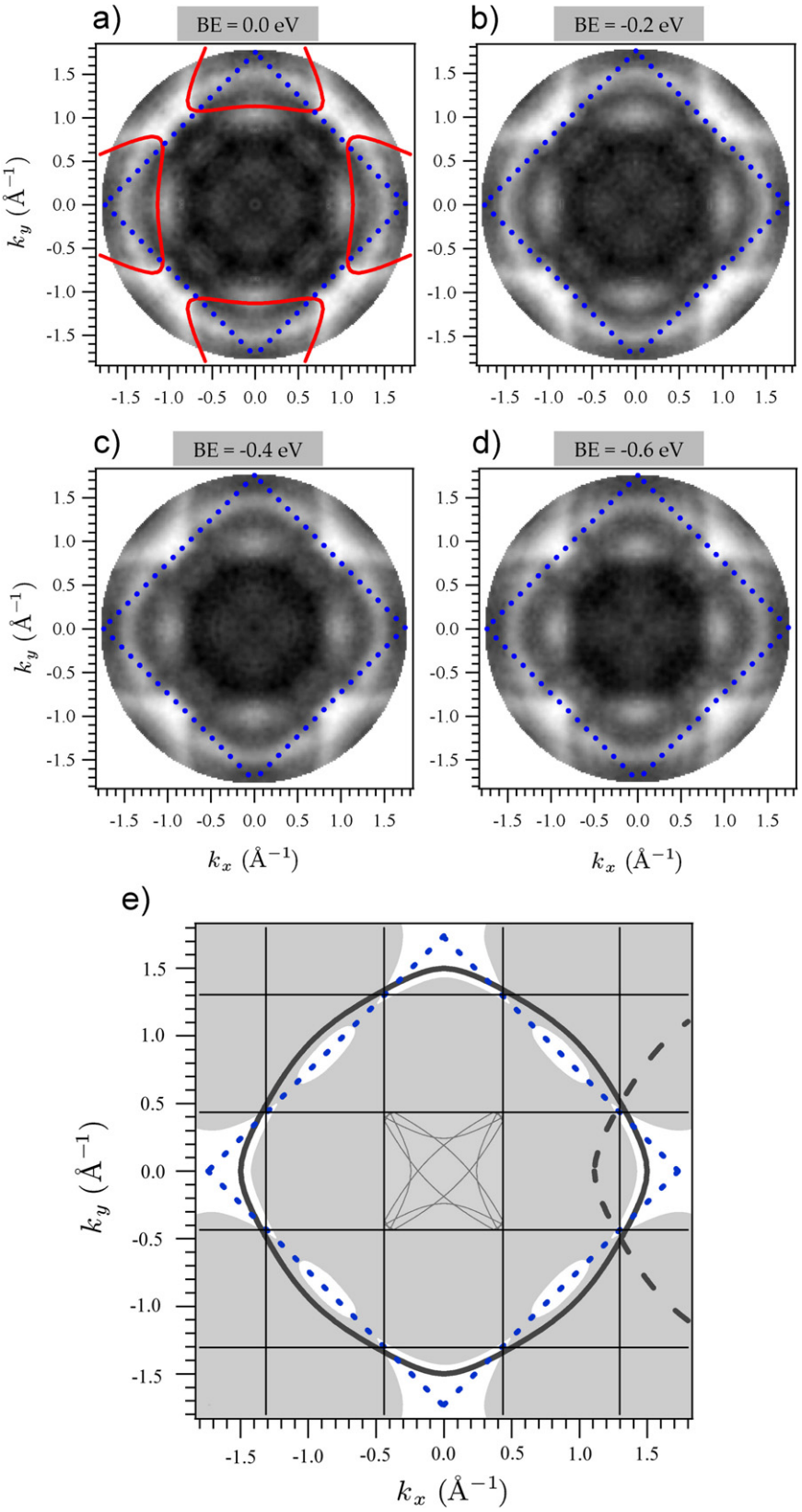

Figure 5. (a)–(d) Constant binding energy surfaces for BE = 0.0 (Fermi contour), −0.2, −0.4 and −0.6 eV for the $(2\sqrt{2} \times 2\sqrt{2})$R45° phase. Photoemission intensity is represented in a logarithmic gray scale. The (1 × 1) first Brillouin zone is drawn with dotted lines. The red (gray) lines in panel (a) represent the calculated Cu(100) bulk constant energy surface projection for the photon energy used [22]. Panel (e) shows a scheme of the observed folding of the surface band. The gray background corresponds to the band bulk projection along the (100) face, leaving absolute gaps represented as white areas. Continuous lines mark the $(2\sqrt{2} \times 2\sqrt{2})$R45° Brillouin zone edges and a dotted line the (1 × 1) Brillouin zone edge. A black quasi-circular line represents the surface state Fermi contour, which is repeated with $(2\sqrt{2} \times 2\sqrt{2})$R45° periodicity. The full $(2\sqrt{2} \times 2\sqrt{2})$R45° folding is shown only for the central Brillouin zone. The folded band observed in the experiment is shown as a quasi-circular dashed line.

value. The value of k_F is simply related to the electronic density n_{2D} as $k_F = \sqrt{2\pi n_{2D}}$, which gives a nominal value of 3.58×10^{15} electrons cm^{-2} for the 0.625 ML phase, providing $\approx$18.6 electrons per $2\sqrt{2}$ unit cell. A similar value is reached from m^* and E_0. The number of electrons per unit cell can also be calculated more precisely by measuring the experimental area of the Fermi contour (which is not exactly a circle) and comparing it to the unit cell size in reciprocal space. A value of 16.5 electrons per unit cell is obtained for the $2\sqrt{2}$ unit cell. However, this number is smaller than the 20 electrons' nominal value (for the five Sn atoms), suggesting that only four Sn are providing charge. Interestingly, this is the number of Sn atoms more tightly bonded, as previously discussed.

An analysis of the energy dependence of the constant energy contours reveals several interesting features. The Fermi energy contour is fairly uniform, showing no apparent gap opening at any accessible area of reciprocal space. The data from figure 5 demonstrate that the zone edge bandgap does not reach the Fermi energy, at least in the accessible reciprocal space areas. This is at variance with the behavior observed for the similar surface band in In/Cu(100)-$(2\sqrt{2} \times 2\sqrt{2})$R45°, where a bandgap opens at the Fermi energy when the band reaches the $(2\sqrt{2} \times 2\sqrt{2})$R45° zone edge [11].

The nature of the Sn/Cu(100) phase transition and the changes in the electronic structure observed can be compared to the phase transitions recently discovered for In/Cu(100) [9, 10], from a $(9\sqrt{2} \times 2\sqrt{2})$R45° reconstruction at RT to a $(\sqrt{2} \times \sqrt{2})$R45° phase above ~350 K, and from a $(2\sqrt{2} \times 2\sqrt{2})$R45° at RT to a p(2 × 2) above 405 K. Concerning the first phase transition, the observation in the case of Sn/Cu(100) of a free-electron-like surface state related to the phase transition indicates that it might be a more general phenomenon, and that other metal/Cu(100) interfaces, which also exhibit $(n\sqrt{2} \times m\sqrt{2})$R45° reconstructions, could also undergo similar temperature-induced phase transitions. However, at variance with the excellent nesting observed in the Sn/Cu(100) case, the nesting condition is less well satisfied in the case of In/Cu(100), because the nested areas are related by a $2k_F$ vector that does not agree with the periodic lattice distortion. Thus, besides Fermi surface nesting, we expect that other driving forces, like strain, may play a crucial role in some of the reconstructions found on Cu(100). On the other hand, the $(2\sqrt{2} \times 2\sqrt{2})$R45°-Sn/Cu(100) phase does not exhibit any temperature-induced phase transition, at variance with the same phase for In/Cu(100). The electronic behavior found for the equivalent phase in Sn/Cu(100) indicates that no electronic contribution is expected in this case, since the zone edge bandgap is observed well below the Fermi energy. This is at variance with In/Cu(100), where the bandgap reached the Fermi level at some areas of reciprocal space, thus supporting the dual nature found for the In/Cu(100) phase transition [11].

We conclude that $(2\sqrt{2} \times 2\sqrt{2})$R45°-Sn/Cu(100) presents a surface band similar to other Sn/Cu(100) and In/Cu(100) phases. Its surface electronic structure is understood assuming a simple folding of this band. Avoided-crossing bandgaps are detected always below the Fermi energy. No surface phase transition was found for this structure.

Acknowledgments

We acknowledge financial support by the Spanish MEC (FIS2005-00747 and FIS2007-29085-E) and by CAM (S-0505/PPQ/0316). Work at Elettra is supported by the EU under contract RII3-CT-2004-506008 (IA-SFS).

References

[1] van Gastel R *et al* 2000 *Nature* **408** 665
[2] Argile C and Rhead G E 1983 *Surf. Sci.* **135** 18
[3] McLoughlin E, Cafolla A A, AlShamaileh E and Barnes C J 2001 *Surf. Sci.* **482–485** 1431
[4] Cafolla A A, McLoughlin E, AlShamaileh E, Guaino Ph, Sheerin G, Carty D, McEvoy T, Barnes C, Dhanak V and Santoni A 2003 *Surf. Sci.* **544** 121
[5] Pussi K, AlShamaileh E, McLoughlin E, Cafolla A A and Lindroos M 2004 *Surf. Sci.* **549** 24
[6] Martínez-Blanco J, Joco V, Segovia P, Balasubramanian T and Michel E G 2006 *Appl. Surf. Sci.* **252** 5331
[7] Nara Y, Yaji K, Iimori T, Nakatsuji K and Komori F 2007 *Surf. Sci.* **601** 5170
[8] Lallo J, Goncharova L V, Hinch B J, Rangan S, Bartynski R A and Strongin D R 2008 *Surf. Sci.* **602** 2348
[9] Nakagawa T, Boishin G I, Fujioka H, Yeom H W, Matsuda I, Takagi N, Nishijima M and Aruga T 2001 *Phys. Rev. Lett.* **86** 854
[10] Nakagawa T, Mitsushima S, Okuyama H, Nishijima M and Aruga T 2002 *Phys. Rev.* B **66** 085402
[11] Nakagawa T, Okuyama H, Nishijima M, Aruga T, Yeom H W, Rotenberg E, Krenzer B and Kevan S D 2003 *Phys. Rev.* B **67** 241401(R)
[12] Martínez-Blanco J, Joco V, Ascolani H, Tejeda A, Quirós C, Panaccione G, Balasubramanian T, Segovia P and Michel E G 2005 *Phys. Rev.* B **72** 041401
[13] Martínez-Blanco J, Joco V, Fujii J, Segovia P and Michel E G 2008 *Phys. Rev.* B **77** 195418
[14] Bauer E 1987 *Structure and Dynamics of Surfaces II* (*Springer Topics in Current Physics* vol 43) ed V Schommers and P von Blanckenhagen (Berlin: Springer)
[15] Persson B N J 1992 *Surf. Sci. Rep.* **15** 1
[16] Mascaraque A and Michel E G 2002 *J. Phys.: Condens. Matter* **14** 6005
[17] Tosatti E 1995 *Electronic Surface and Interface States on Metallic Systems* ed E Bertel and M Donath (Singapore: World Scientific)
[18] Aruga T 2002 *J. Phys.: Condens. Matter* **14** 8393
[19] Aruga T 2006 *Surf. Sci. Rep.* **61** 283
[20] Pussi K, McEvoy T, Barnes C J, Cafolla A A, AlShamaileh E and Lindroos M 2003 *Surf. Sci.* **526** 141
[21] Hatta S, Walker C J, Sakata O, Okuyama H and Aruga T 2004 *Surf. Sci.* **565** 144
[22] Joco V, Mikuszeit N, Martinez-Blanco J and Michel E G 2009 at press